Breeding Science *Preview*
doi: 10.1270/jsbbs.24067

Research Paper

Detection and validation of QTLs for flowering time in morning glory

Hiroaki Katsuyama[1,2], Takuro Ito[1], Kyousuke Ezura[1], Emdadul Haque[1], Atsushi Hoshino[3,4], Eiji Nitasaka[5], Michiyuki Ono[2,6], Shusei Sato[7], Sachiko Isobe[7], Hiroyuki Fukuoka[8,9], Nobuyoshi Watanabe[1] and Tsutomu Kuboyama*[1]

[1] *College of Agriculture, Ibaraki University*, 3-21-1 Chuo, Ami, Ibaraki 300-0393, Japan
[2] *Institute of Life and Environmental Sciences, University of Tsukuba*, 1-1-1 Tennodai, Tsukuba, Ibaraki 305-8572, Japan
[3] *National Institute for Basic Biology*, Okazaki, Aichi 444-8585, Japan
[4] *Graduate Institute for Advanced Studies, SOKENDAI*, Okazaki, Aichi 444-8585, Japan
[5] *Department of Biological Science, Graduate School of Science, Kyushu University*, 744 Motooka, Nishi-ku, Fukuoka 819-0395, Japan
[6] *Gene Research Center, Tsukuba-Plant Innovation Research Center (T-PIRC), University of Tsukuba*, 1-1-1 Tennodai, Tsukuba, Ibaraki 305-8572, Japan
[7] *Kazusa DNA Research Institute*, 2-6-7 Kazusa Kamatari, Kisarazu, Chiba 292-0818, Japan
[8] *National Institute of Vegetable and Tea Science, National Agriculture and Food Research Organization*, 360 Kusawa, Ano, Tsu, Mie 514-2392, Japan
[9] *Present address: Plant Breeding and Experiment Station, Takii & Co., Ltd.*, Konan, Shiga 520-3231, Japan

Japanese morning glory (*Ipomoea nil*), a short day plant, has been used for studying flowering times. Here, quantitative trait loci (QTL) analysis for days from sowing to flowering (DTF) of F_2 between *I. nil* var. Tokyo Kokei Standard (TKS) and *I. hederacea* line var. Q65, an early flowering variety, revealed seven QTLs: *QTL Ipomoea Flowering 1–7* (*qIF1–7*). The position of *qIF3*, which had the most significant effect among the seven QTLs, corresponds with that of *I. nil* (or *I. hederacea*) *CONSTANS* (*InCO/IhCO*) in the linkage map. There is a single-base InDel in the coding sequence of *InCO/IhCO*. The single-base deletion (SBD) causes a frame-shift mutation and loss of function in TKS allele (*inco-1*). *I. nil* accessions bearing *inco-1* tend to flower early, similarly to rice varieties bearing the loss of function allele of *CO* ortholog, *hd1*. The TKS allele of *qIF3* reduces DTF and corresponds with the inferred effect of *inco-1*. Based on the distribution of *inco-1*, a hypothesis was proposed that the SBD in *inco-1* might have played an important role in the expansion of Japanese morning glories, originally native to the tropical regions of the Americas, into temperate Asia.

Key Words: *CONSTANS*, flowering time, *Ipomoea nil*, *Ipomoea hederacea*, QTL, short day plants, adaptation.

Introduction

Japanese morning glory (*Ipomoea nil*), a short-day (SD) plant that is highly sensitive to the photoperiod, has been used as a model plant to study flowering (Hayama *et al.* 2007, Higuchi *et al.* 2011, Takeno 2016). Genetic pathways that promote flowering in response to seasonal cues were first reported in the model species *Arabidopsis thaliana* (Andrés and Coupland 2012), a long-day (LD) plant in which *CO* expression is regulated by light. The circadian clock plays a central role in regulating photoperiodic flowering (Andrés and Coupland 2012). *CO* encodes a zinc finger transcription factor, which binds to the promoter of *FLOWERING LOCUS T* (*FT*), a florigen gene, and which positively affects *FT* expression (Cao *et al.* 2014, Putterill *et al.* 1995).

For SD plants, intensive genetic studies of flowering have been conducted in rice (Hori *et al.* 2016). Several genes key to controlling the heading date of rice have been identified using quantitative trait locus (QTL) analysis and have been cloned. *Heading date 1* (*Hd1*), the ortholog of Arabidopsis *CO*, is a major gene controlling the heading date in rice (Yano *et al.* 2000). In fact, *Hd1* regulates expression of the *Heading date 3a* (*Hd3a*) rice florigen gene, delays heading under LD, and promotes heading under SD (Hayama *et al.* 2003, Izawa *et al.* 2002, Kojima *et al.* 2002, Tamaki *et al.* 2007, Yano *et al.* 2000).

From the study of *I. nil* flowering, the homologous genes

Communicated by Kyoko Kawakatsu
Received September 6, 2024. Accepted June 25, 2025.
First Published Online in J-STAGE on October 15, 2025.
*Corresponding author (e-mail: tsutomu.kuboyama.a@vc.ibaraki.ac.jp)

of *Arabidopsis* flowering genes have been isolated (Hayama *et al.* 2007, Higuchi *et al.* 2011, Liu *et al.* 2001, Zheng *et al.* 2009). The *I. nil CO* ortholog, INIL11g18779, was originally named *PnCO* because of the former scientific name of Japanese morning glory: *Pharbitis nil*. As presented herein, the prefix "*Pn*" of genes derived from *I. nil* is replaced with "*In*". Therefore, *PnCO* will be referred to as *Ipomoea nil CONSTANS* (*InCO*) herein. *InCO*, which is highly expressed in SD condition, has multiple splicing variants: a transcript containing a long intron (*InCO* (li)), a transcript containing a short intron (*InCO* (si)), and a transcript containing no intron (*InCO* (ni)) (Liu *et al.* 2001). Only the *InCO* (ni) mRNA encodes complete CONATANS-like protein with a CO, CO-like TOC1 (CCT) domain. It can restore an *Arabidopsis co* mutant. By contrast, *InCO* (li) and *InCO* (si) encodes truncated protein lacking the terminal CCT domain (Liu *et al.* 2001). Two *I. nil* homologous genes of *FT*, *PnFT1* and *PnFT2*, expressed only in inductive SD conditions and overexpression of *PnFT1*, promote flowering in *Arabidopsis* and *I. nil* (Hayama *et al.* 2007). Transgenic plants constitutively expressing *I. nil* ortholog of *GIGANTEA*, *PnGI*, form fewer flowers than non-transgenic plants do. However, the expression level of *InCO* does not differ dramatically in transgenic plants compared to non-transgenic plants (Higuchi *et al.* 2011). Consequently, although the homologous genes of flowering related genes in *Arabidopsis* have been reported in *I. nil*, their function in photoperiodic flowering remains unclear.

The whole genome sequence of *I. nil* 'Tokyo Kokei Standard' (TKS) has been sequenced and useful genome sequences are now available (Hoshino *et al.* 2016a). EST-SSR marker of *I. nil* has also been reported: approximately half of them are polymorphic between TKS and Ivy-leaved morning glory, *I. hederacea* 'Q65' (Q65) (Ly *et al.* 2012). In addition, single nucleotide polymorphisms (SNP) become easily detected by comparing mRNA sequences between two accessions using the next generation sequencing (NGS) (Edwards *et al.* 2012). Although interspecific hybridizations between Q65 and Japanese strains of *I. nil* is not easy and reported that two pods and three seeds were obtained by pollination using 22 flowers (Yoneda and Takenaka 1981), F_1 hybrids are fertile and F_2 population is applicable to construct linkage maps. Consequently, these techniques and plant materials enable us to map QTLs for days from sowing to flowering (DTF) in morning glory.

Actually, *I. nil* has varieties of various flowering times (Yoneda and Takenaka 1981). Consequently, natural variations in *I. nil* are attractive resources for mapping QTLs affecting flowering time in dicot SD plants. Flowering in late July in Ibaraki, Japan, TKS is a standard variety of Japanese morning glory. Q65 was probably transported from the United States to Japan along with grains. It blooms approximately two weeks earlier than TKS. This report describes QTL mapping of DTF in the F_2 population between Q65 and TKS and a frame-shift mutation found in the TKS allele of *InCO*, which is the candidate gene of the most prominent QTL of DTF.

Materials and Methods

Plant materials

I. nil accessions TKS (Q1065), Q31, Q33, Q61, Q62, Q63, and Q1187 and an *I. hederacea* accession, Q65, and the F_2 population derived from the interspecific cross Q65 × TKS were provided by the Morning glory stock center of Kyushu University with support by the National Bio-Resource Project of the MEXT, Japan. An *I. nil* accession, PI227365 was provided by Agricultural Research Service, United States Department of Agriculture. *I. nil* varieties, Pekin-tendan (PKT) and Yakuyou-shirohana (YYS) were derived from the genetic stock of Ibaraki University (Hoshino *et al.* 2016b). An *I. nil* variety, Violet, was purchased from Marutane Seed Co., Kyoto, Japan. After dividing 192 individuals from the F_2 population, each of the 96 individuals was cultivated in 2011 and 2012. These plants were cultivated under natural conditions at the College of Agriculture, Ibaraki University (36°2′14″N, 140°12′47″E), Ami, Ibaraki, Japan.

SSR marker development from I. nil and I. batatas

Using 10% acrylamide gel electrophoresis, 326 SSR markers from *I. nil* (Ly *et al.* 2012) and 1250 EST-SSR markers from *I. batatas* (Kazusa DNA Lab, Japan) were analyzed. Polymorphic markers between TKS and Q65 were selected for genotyping the F_2 population (**Supplemental Table 1**). DNA was extracted from fresh leaves of each plant using a DNeasy Plant Mini kit (Qiagen Inc.). Each 6 µl of reaction mixture contained 1xNH_4 reaction buffer (Bioline; Meridian), 0.2 mM dNTP, 3 mM $MgCl_2$, 0.2 µM each primer, 0.15 unit *Taq* polymerase (Bioline; Meridian) and 1.0 ng of template DNA. Polymerase chain reactions (PCR) were run using a modified 'touchdown PCR' program (Sato *et al.* 2005). EST-SSR markers derived from *I. nil* (Ly *et al.* 2012) and *I. batatas* (**Supplemental Table 1**) showing polymorphisms between Q65 and TKS in polyacrylamide gel electrophoresis were used for linkage-maps construction.

Development and genotyping of SNP markers

After mRNA was isolated from 0.1 g buds of Q65 using an RNeasy Plant mini kit (Qiagen Inc.), it was sequenced using a Genetic Analyzer II (Illumina Inc.). Using software (Maq; Li *et al.* 2008), the sequence reads were mapped to a reference sequence, the non-redundant *I. nil* ESTs derived from TKS buds cDNA (Hoshino *et al.* 2016a, Ly *et al.* 2012), and were used to detect SNPs between Q65 and TKS. The detected SNPs were then used to develop SNP markers.

The RNA-seq data were archived at the DNA Data Bank of Japan under accession number DRA010196. These SNPs were genotyped by high-resolution melting (HRM) analysis (Liew *et al.* 2004) or melting temperature (T_m)-shift primer

method (Fukuoka *et al.* 2008, Wang *et al.* 2005). Primers for HRM analysis were designed with Primer 3 (Rozen and Skaletsky 2000) (**Supplemental Table 2**). In designing of primers for HRM, Primer 3 parameters of PCR-amplicon length, optimal melting temperature, and primer length were set respectively as 80–110 bp, 60°C, and 20 bases. PCR amplification and DNA melt curve analysis were performed in a total volume of 10 µl containing 10 mM Tris-HCl (pH 8.3), 65 mM KCl, 1.5 mM $MgCl_2$, 0.2 µM each primer, 0.2 mM dNTP, 1.25% glycerol, 0.4× Eva Green (Biotium Inc.), 0.25 U *Taq* DNA polymerase (Ampliqon AS) and 1.0 ng of template DNA (Fukuoka *et al.* 2008). The PCR for HRM analysis was performed in High Resolution Melt/DNA binding Dye/DNA/PCR with HRM Curve mode of the Eco real-time PCR system (Illumina Inc.). The PCR conditions were 94°C for 3 min, 40 cycles of 96°C for 20 s, 58°C for 1 min, and 72°C for 30 s followed by melt curve analysis using the default settings of the system.

Primers for T_m-shift primer method were designed using 'tms_primer_designer.pl' (Fukuoka *et al.* 2008) (**Supplemental Table 3**). The PCR for Tm-shift primer method was performed in Quantification/DNA binding Dye/Standard curve mode of an Eco real-time PCR system (Illumina Inc.). The PCR conditions were 94°C for 3 min, 40 cycles of 95°C for 20 s, 58°C for 30 s, and 72°C for 30 s with subsequent melt curve analysis using the default settings of the system.

Linkage map construction and QTL analysis

From genotyping data of the F_2 population, we constructed linkage maps using QTL IciMapping software ver. 4.2 (Meng *et al.* 2015) and MapChart software (Voorrips 2002). DTF was calculated from the date of sowing to the date on which the first flower of an individual plant opened. Using each constructed linkage map and DTF-trait data, we detected QTLs for DTF with R/qtl package (Broman *et al.* 2003). We conducted interval mapping and composite interval mapping, respectively using the function, "scanone" and "cim". Multiple QTL models were constructed by "scantwo", "makeqtl", "fitqtl", "refineqtl" and "stepwiseqtl". To establish alpha = 0.05 significant thresholds, the data were permutated 1000 times in each experiment. The estimated percent variances explained for the QTL and effects of QTL were calculated using the function "fitqtl".

PCR amplification and DNA sequencing of the Q65 ortholog of InCO (IhCO)

Four primer sets were used for PCR amplification of *IhCO* and its 5′ flanking region (**Supplemental Table 4**). PCR amplifications were performed using KOD FX Neo DNA polymerase (Toyobo Co. Ltd., Osaka, JAPAN). The nucleotide sequences of the PCR products were analyzed with a capillary sequencer (ABI3130; Life Technologies Inc.) using the primers presented in **Supplemental Table 4**. The DNA sequence data derived from *IhCO* were archived at the DNA Data Bank of Japan under accession nos. LC716650 and LC768960. The alignments of nucleotide sequences and putative amino-acid sequences were found using Clustal W ver. 2.1 (Larkin *et al.* 2007). Splicing site prediction was performed with NetGene2-2.42 server (Hebsgaard *et al.* 1996, https://services.healthtech.dtu.dk/services/NetGene2-2.42/).

Quantitative reverse transcription PCR (qRT-PCR) analysis

TKS and Q65 plants were cultivated at 25°C under continuous light (195 µmol $m^{-2}s^{-1}$) until five days after sowing and were grown under SD (10 h light/14 h dark) or LD (14 h light/10 h dark) conditions for 3 days. Then, cotyledons were harvested after treating 8 h or 14 h of dark period from the last light period. Total RNA was isolated from cotyledons using an SV Total RNA Isolation System (Promega Corp.). cDNA was synthesized using Prime Script RT Master mix (Takara Bio Inc.). Real-time PCR was conducted using a Light Cycler 96 system (Roche) with TB Green® *Premix Ex Taq*™ II (Takara Bio Inc.). Three primer sets, ni (forward primer (Fwd) 5′-AGGGACT GCAGCAGCATAAC-3′ and reverse primer (Rev) 5′-TGG AGACCATATCCCGTGTT-3′), si (Fwd 5′-CCATCAGTC ACACAGTCTCCA-3′ and Rev 5′-TGAAGCTGTGGAGG CATCTG-3′) and li (Fwd 5′-TCCAATAAAACCCAACGT CA-3′ and Rev 5′-GGGGAAGTTGCATACCTTGA-3′), were designed and used for qRT-PCR analyses of three *InCO/IhCO* splicing variants. The primer set for *InACTIN4* (Fwd 5′-GAATACTTGTATGCCACGAGCA-3′ and Rev 5′-GGATTGCCAAGGCAGAGTAT-3′) was used as the internal reference gene. Real-time PCR conditions were 94°C for 3 min, 40 cycles of 95°C for 10 s, 58°C for 30 s, and 72°C for 15 s, followed by melt curve analysis using default settings of the system. Relative expression levels for each sample were calculated based on the comparative Ct method. Welch's two-tailed *t*-test was used to compare the expression levels between TKS and Q65.

Results

DTF in F_2 populations

In 2011 and 2012, seeds of the F_2 population were sown respectively on May 20 and June 7. The DTF values of individuals were measured (**Fig. 1**): those for Q65 and TKS were, respectively, 54 and 62 days in 2011 and 38 and 52 days in 2012. The ranges of DTF in the F_2 populations of 2011 and 2012 were 46–80 days and 39–76 days, respectively; more than half of individuals flower later than both parents in 2012 (**Fig. 1**).

Marker development and linkage-map construction

The F_2 populations cultivated in 2011 and 2012 were genotyped by DNA markers for constructing genetic linkage maps. The linkage map of the 2011 population contained 250 loci including 53 Tm-shift-SNP markers, 37

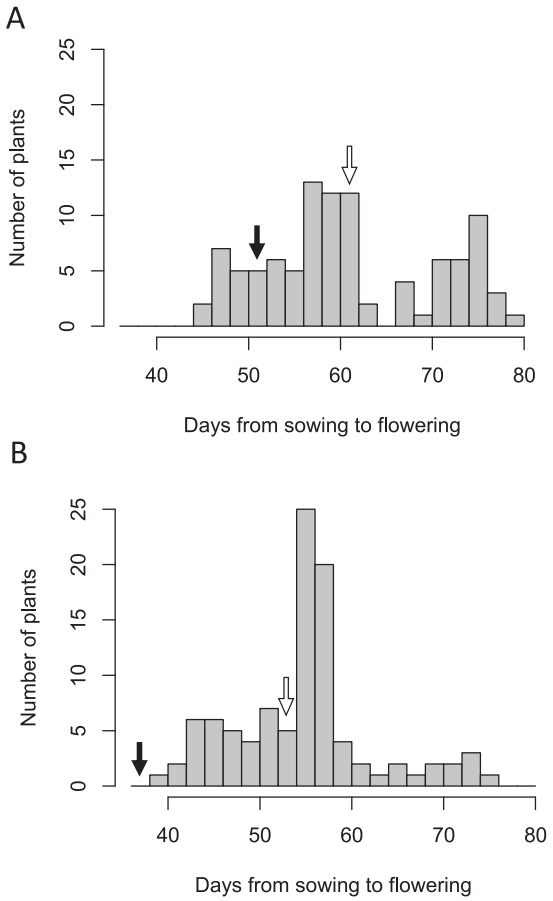

Fig. 1. Distribution of days from sowing to flowering among F_2 population derived from a cross: Q65 × TKS. A and B respectively show the F_2 population in 2011 and 2012. The black arrow and white arrow respectively indicate flowering days of Q65 and TKS.

HRM-SNP markers, 143 EST-SSR markers of *I. nil*, 16 EST-SSR markers of *I. batatas* and one phenotypic marker, covered a total length of 1799 cM and included 15 linkage groups (**Supplemental Fig. 1**, **Supplemental Tables 1–3**). The linkage map of the 2012 population contained 192 loci including 43 Tm-shift-SNP markers, 34 HRM-SNP markers, 97 EST-SSR markers of *I. nil*, 17 EST-SSR markers of *I. batatas* and one phenotypic marker, covered a total length of 1664 cM and consisted of 15 linkage groups (**Supplemental Fig. 2**, **Supplemental Tables 1–3**). These constructed linkage groups were anchored to chromosomes using pseudo-chromosomes of Asagao_1.1 (Hoshino *et al.* 2016a) (**Supplemental Figs. 1**, **2**).

QTL analysis for DTF

In the F_2 population cultivated in 2011, four QTLs for DTF, designated as *qIF1*, *qIF2*, *qIF3*, and *qIF4* were mapped in the vicinity of the DNA marker of IES0160 on chromosome 5, Contig11987 on chromosome 9, Contig4567.156 on chromosome 11, and Contig05575 on chromosome 14 based on a multiple QTL model, respectively (**Table 1**, **Supplemental Figs. 1**, **3**, **4**). In this QTL model, the phenotype y is modeled as y = *qIF1* + *qIF2* + *qIF3* + *qIF4* + *qIF1*:*qIF4* (A colon between two QTLs denotes interaction between the QTLs). The percentage of phenotypic variance explained (PVE) by these QTLs was 14.5%–23.1% (**Table 1**); the total PVE was 73.7% based on the multiple QTL model.

In the F_2 population cultivated in 2012, a multiple QTL model was obtained consisting of three QTLs other than *qIF3*. The three QTLs, *qIF5*, *qIF6*, and *qIF7* were mapped in the vicinity of the DNA marker of rJMFF041I11 on chromosome 4, Contig683.0110 on chromosome 10, and JMFN020H15 on chromosome 14, respectively (**Table 1**, **Supplemental Figs. 2**, **3**, **5**). In this QTL model, the phenotype y is modeled as y = *qIF3* + *qIF5* + *qIF6* + *qIF7* + *qIF6*:*qIF7*. The PVE by these QTLs was 6.3%–27.3% (**Table 1**); the total PVE was 58.4% based on the multiple QTL model.

qIF3 showed the highest PVE among these QTLs (23.1%) in the 2011 analysis and demonstrated stability by being detected as a significant QTL again in 2012. However, the LOD value of *qIF3* in 2012 was reduced by approximately one-third compared to that in 2011. The *qIF1*

Table 1. Multiple QTL mapping of DTF in the cross between Q65 and TKS

QTL name	Year	Nearest marker	Chr.	Position (cM)	99% CI[a] (cM)	LOD	%var[b]	*a*[c] SE[d]	*d*[e] SE	P (F)
qIF1	2011	IES0160	5	37	29–42	10.0	16.2	–5.4 ± 0.9	0.5 ± 1.2	3.2E-07
qIF2	2011	Contig11987	9	10	2–17	10.7	17.6	6.0 ± 1.4	–3.1 ± 1.4	5.7E-10
qIF3	2011	Contig4567.156	11	28	25–34	13.1	23.1	6.9 ± 0.9	4.2 ± 1.2	4.4E-12
	2012	Contig4567.156	11	50	37–64	5.6	13.0	4.2 ± 0.8	0.9 ± 1.5	1.4E-05
qIF4	2011	Contig05575	14	16	10–20	9.1	14.5	–4.6 ± 1.0	1.8 ± 1.2	1.1E-04
qIF1:*qIF4*[f]	2011	–	–	–	–	6.2	9.2	–	–	4.8E-05
qIF5	2012	rJMFF041I11	4	43	0–72	2.9	6.4	–3.3 ± 0.9	0.4 ± 1.2	2.9E-03
qIF6	2012	Contig683.0110	10	88	83–91	10.4	27.3	–4.0 ± 0.8	–1.9 ± 1.2	1.6E-07
qIF7	2012	JMFN020H15	14	42	34–54	10.2	26.5	–1.1 ± 1.0	–3.5 ± 1.3	2.4E-07
qIF6:*qIF7*	2012	–	–	–	–	8.9	22.4	–	–	3.3E-07

[a] 99% CI, 99% Bayesian credible interval of the QTL; [b] %var, percentage of variance explained by the QTL; [c] a, additive effect; [d] SE, standard error; [e] d, dominance effect; [f] Colons show interactions between two QTLs.

and *qIF2* also demonstrated the readily apparent effects (**Table 1**, **Supplemental Fig. 4**) and detected in the simple interval mapping (SIM) or the composite interval mapping (CIM) (**Supplemental Fig. 3**). However, no QTLs except *qIF3* were detected neither in SIM and CIM in 2012 analysis (**Supplemental Fig. 3**). In 2012, seeds were sown two weeks later than in 2011. The shorter period of long-day condition in 2012 population might reduce power for detection of QTL related to photoperiodism.

qIF1 and *qIF4* in 2011 and *qIF6* and *qIF7* in 2012 were detected as interacting QTLs (**Supplemental Fig. 6A–6C**). In individuals with a homozygous Q65 allele of *qIF7*, the plants that are homozygous for the TKS allele of *qIF6* exhibited a delayed flowering compared to plants homozygous and heterozygous for the Q65 allele of *qIF6* (**Supplemental Fig. 6C**). A significant interaction (LOD = 7.12 > 6.39 ($P = 0.05$)) was also detected between the chromosomal region at 116 cM of chromosome 14 (14@116) and at 123 cM of chromosome 5 (5@123) (**Supplemental Fig. 6D**). The effects of TKS and Q65 allele of 5@123 reversed depending on 14@116 genotypes.

Polymorphism between the TKS and Q65 alleles of InCO/IhCO

The strongest effect QTL for DTF, *qIF3* was co-located with *InCO/IhCO* in the linkage maps. Also, Contig4567.156, the DNA marker the nearest to the LOD peak of *qIF3*, was developed based on polymorphism in the EST encoding *InCO* (**Table 1**, **Supplemental Figs. 1**, **2**, **Supplemental Table 2**). Additionally, when we searched the confidence interval of *qIF3* using the Japanese morning glory genome database, no homologs of genes related to flowering time in other plant taxa, except for *InCO*, were identified. Consequently, *InCO/IhCO* might be a candidate of *qIF3*. Therefore, we compared the DNA sequence of *InCO/IhCO* between TKS and Q65.

First, using PCR amplification and agarose gel electrophoresis, the 5′ flanking regions of *InCO/IhCO* were compared among Q65 and four *I. nil* accessions: PKT, TKS, Q63, and YYS (**Fig. 2**). The size of PCR products amplified from Q65 was 2.3 kbp and approximately 300 bp larger than that of other accessions (**Fig. 2**), which is attributable to the structural difference of the 5′ flanking region of *InCO/IhCO* between Q65 and other accessions including TKS. Then, the PCR products of Q65 were sequenced and aligned with the DNA sequence of TKS (Hoshino *et al.* 2016a) (**Supplemental Fig. 7**). Short interspersed element (SINE)-like 168 bp insertion sequence was found in the reverse strand of approximately 1.9 kb upstream of the putative transcription start site (**Supplemental Fig. 7**). There were a conserved putative RNA polymerase III promoter containing A-box and B-box (Galli *et al.* 1981) and target site duplications (**Fig. 3**). A few thousand copies of this SINE-like sequence were detected by homology search against the Asagao 1.2 genome (Hoshino *et al.* 2016a) using the BLAST program. DNA

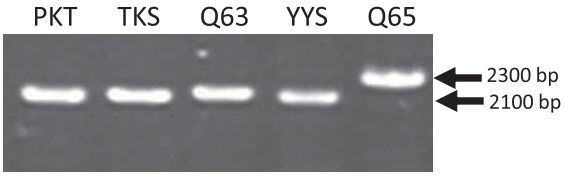

Fig. 2. Agarose gel electrophoresis of PCR products amplified from the 5′ flanking regions of *InCO/IhCO* in five morning glory accessions: PKT, Pekin tendan; TKS, Tokyo Kokei standard; Q63; YYS, Yakuyo shirohana; and Q65.

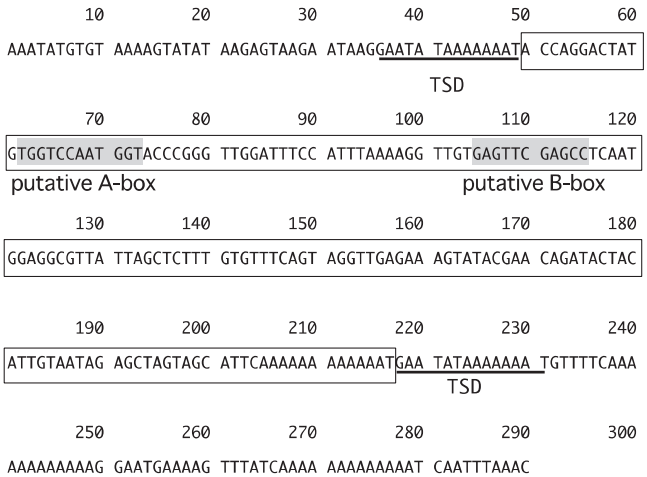

Fig. 3. A SINE-like sequence found in the 5′ flanking region of *IhCO*. DNA sequences surrounded by square frame show the SINE-like sequence. TSD, target site duplication. TSDs are shown by underlining. The locations of putative boxA and boxB are shown by a gray background.

sequences downstream of the SINE-like sequence were highly polymorphic between TKS and Q65. There was a long TA repeat (more than 200 bp) in the Q65 sequence (**Supplemental Fig. 7**).

In addition to the polymorphisms in the 5′ flanking region, the coding sequence (CDS) of Q65 had 10 single-base substitutions (SBS) and 3 insertions against TKS sequence. Of the 10 SBSs, 7 are synonymous substitutions, which represent functional constraints of *InCO/IhCO*. Of the three insertions, the two insertions were 9 and 12 nucleotides, causing an additional 3 and 4 amino acids, respectively, but one was a single-base insertion causing a frame-shift of the translational reading frame (**Fig. 4A**). The Q65 allele has a single cytosine base present between positions 7617445 and 7617446 on Chr11 of TKS in the genome sequence (Asagao_1.2) (**Fig. 4A**). If the splice sites are identical to *InCO* (ni), the transcript reported for the 'Violet' allele (Liu *et al.* 2001), then the Q65 mRNA would encode an incomplete protein without a CCT domain due to the insertion. Therefore, the splice-donor site of Q65 allele was assessed using NetGene2-2.42 server (Hebsgaard *et al.* 1996) (**Fig. 4B**). As a result, the splice-donor site of *InCO* (ni) was not detected confidently and 26 nucleotides (nt) downstream from the splice-donor site of *InCO* (ni) was the most

A

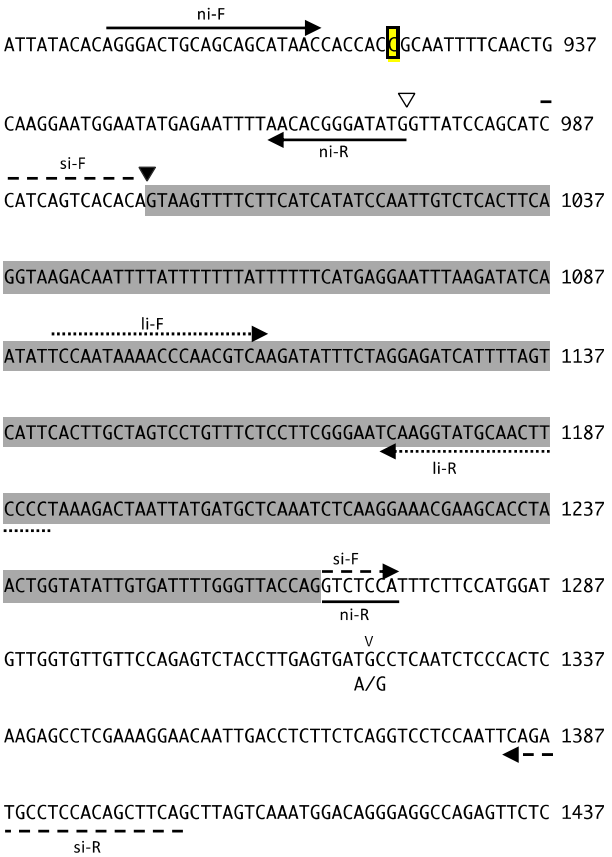

B

Pos.	Confidence	5´ Exon^Intron 3´
1001	1.00	CAGTCACACA^GTAAGTTTTC
1039	0.93	CTCACTTCAG^GTAAGACAAT
1177	0.94	GGGAATCAAG^GTATGCAACT

Fig. 4. *InCO/IhCO*-splice-site prediction at Q65 allele. (A) The genomic DNA sequence around an intron of Q65 allele. Numbers at the right side of DNA sequences show nucleotide numbers from the putative transcription start site. The boxed cytosine is inserted into the TKS allele. A white-reverse triangle shows a splice donor site reported by Liu *et al.* (2001) as no-intron mRNA (*InCO* (ni)). A black reverse triangle shows a splice donor site reported by Liu *et al.* (2001) as short-intron mRNA (*InCO* (si)) and also as predicted by NetGene2 v. 2.4 as the most confident splice-donor site. The DNA sequence with gray background denotes the intron of *InCO* (si). "v" above the DNA sequence signifies the SNP site position. 'A/G' shows the adenine of TKS allele and the guanine of Q65 allele at the SNP site. Primer pairs used for expression analysis are shown as arrows. (B) A splice-donor-site prediction by Net Gene2 v. 2.4. Pos. denotes the nucleotide position from the putative transcription start site.

confident splice-donor site (**Fig. 4B**). The transcript spliced at 26 nt downstream was correspondent with the transcript reported by Liu *et al.* (2001) as *InCO* (si). *InCO* (si) encodes an incomplete protein, which results from premature stop codon in 'Violet' allele (Liu *et al.* 2001), but in the Q65 allele, it encodes complete 433 aa protein with the CCT domain (**Supplemental Fig. 8**).

Distribution of the single-base InDel in the CDS of InCO among accessions derived from natural populations

To determine the ancestral form of the single-base InDel in the CDS of *InCO*, the single-base InDel sites were investigated in eight *I. nil* accessions derived from natural populations in addition to TKS and Q65 (**Table 2**). Accessions Q33 and Q1187, derived from the South American continent, have cytosine insertion at the single-base InDel site as Q65 (**Table 2**). Although the number of accessions surveyed was limited, accessions that have the same sequence as TKS in the single-base InDel are limited to those from the Asian countries (**Table 2**). Since *I. nil* originates from the tropical regions of the Americas (Austin *et al.* 2001), the Q65-type sequence of the single-base InDel is likely to represent the ancestral form. Moreover, the fact that *InCO* orthologs of *Ipomoea* species *I. triloba* and *I. trifida* also contain the Q65-type sequence in the single-base InDel also support the idea that the Q65-type sequence of the single-base InDel is ancestral (**Fig. 5**). Thus, TKS type allele (*inco-1*) might emerged from the ancestral allele of *InCO* (*InCO-2*) by the single-base deletion (SBD) in the CDS (**Fig. 6**).

DTFs of the accessions presented in **Table 2** were investigated in 2022. They were from 44 days of Q65 to

Table 2. DTF and the single-base insertion/deletion in the CDS of *InCO/IhCO* among morning glory varieties

Variety	Origin	Sequence[a]	DTF[b] (± S.E.)	
Q65	–	CCG	44 ± 1.3	*n* = 3
Q61	China	C-G	53 ± 2.9	*n* = 5
Violet	Japan	C-G	60 ± 4.3	*n* = 3
Q62	Nepal	C-G	65 ± 0.7	*n* = 5
TKS	Japan	C-G	66 ± 0.9	*n* = 3
PI227365	Iran	C-G	95 –	*n* = 1
Q31	China	CCG	103 ± 3.6	*n* = 5
Q1187	Paraguay	CCG	109 ± 2.9	*n* = 5
Q63	Guinea	CCG	133 ± 4.1	*n* = 3
Q33	Brazil	CCG	138 ± 1.9	*n* = 4

[a] DNA sequence of the single base insertion/deletion site in the *InCO/IhCO* CDS.
[b] Days from sowing to flowering at Ami, Ibaraki, Japan. Seeds were sown on May 20, 2022.

```
TKS          TAACCACCAC-GCAATTTTCAACTGCAAGGAATGGAATATGAGAATTT
Q65          TAACCACCACCGCAATTTTCAACTGCAAGGAATGGAATATGAGAATTT
I.triloba    TAACCACCACCGCAATTTTCAGCTGCAAGGAATGGAATATGAGAATTT
I.trifida    TAACCAACACCGCAATTTTCAGCTGCAAGGAATGGAATATGAGAATTT
             ****** *** ********** *************************
```

Fig. 5. DNA sequence alignment of *InCO* orthologous genes around the single-base InDel causing frameshift in *InCO*. DNA sequence of *I. triloba* (XR_004098766.1) and of *I. trifida* (CP025648.1) were aligned with Clustal W (Ver. 1.83, 2003). Gray background denotes the single-base-InDel site.

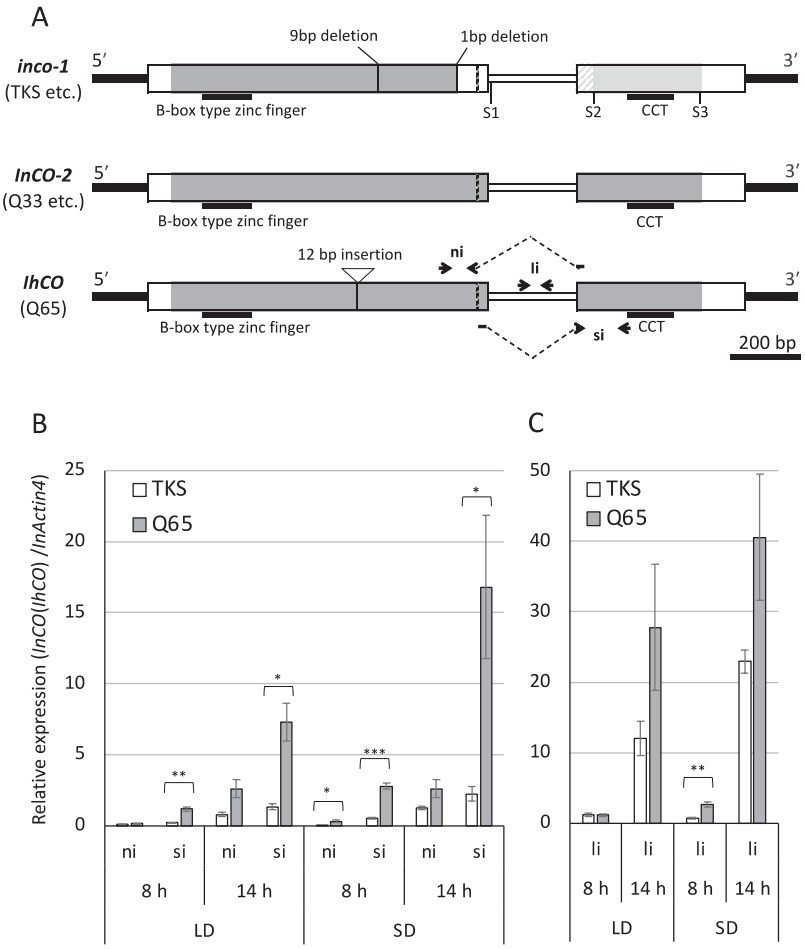

Fig. 6. *InCO/IhCO* alleles and comparison of the expression levels of three transcripts of *InCO/IhCO* in Q65 and TKS. (A) Map of the *InCO/IhCO* alleles and the PCR primer pairs. Narrow black boxes show untranscribed regions. Wider boxes show exons. A narrow white box shows an intron. White triangles and vertical broken lines show cryptic splice sites producing *InCO* (ni). S1, S2, and S3 of *inco-1* respectively show stop codon sites of *InCO* (li), *InCO* (si), and *InCO* (ni). Gray parts of the boxes show regions homologous to IhCO protein in a.a. Light-gray parts of *inco-1* show that InCO (ni) protein is homologous to IhCO protein. The diagonal stripe pattern shows the region where the InCO (ni) protein is homologous with the IhCO protein, but not with the InCO (si) protein. ni, si, and li indicated by arrows and broken lines are primer pairs used for qRT-PCR. These ni, si, and li were used respectively for amplifying splicing variants, *InCO* (ni), *InCO* (si), and *InCO* (li). (B, C) Relative expression analysis of three *InCO* splicing variants using qRT-PCR. *, **, and *** respectively denote significant difference at $P < 0.05$, $P < 0.01$, and $P < 0.001$ by Welch's two-tailed *t*-test).

138 days of Q33. The accessions without the SBD in the CDS of *InCO/IhCO* tended to have longer DTFs than those with the SBD, except for Q65 (**Table 2**).

Comparison of InCO/IhCO expression between TKS and Q65

The expression levels of three transcripts, *InCO* (ni), *InCO* (si), and *InCO* (li) were compared between TKS and Q65 in SD and LD conditions using qRT-PCR (**Fig. 6B**, **6C**). The relative expression levels of the Q65 allele tended to be higher than TKS in all three transcripts across all conditions. Especially, the difference between TKS and Q65 was the most pronounced in *InCO* (si) (**Fig. 6B**). The expression level of *InCO* (si) was sevenfold higher in Q65 than in TKS after 14 h of darkness in the SD condition.

In all conditions, among the transcripts of three types, *InCO* (li) exhibited the highest expression level, as reported earlier in the relevant literature (Liu *et al.* 2001), followed by *InCO* (si). The lowest expression level was observed for *InCO* (ni) (**Fig. 6B**, **6C**). Although quantities differed among the three transcripts, the expression patterns responding to the day length and the dark period were mutually similar. These tendencies were observed for both TKS and Q65.

When comparing expression levels of the transcripts encoding the InCO protein with an intact CCT domain at 14 h after dark in the SD condition, the expression level of *InCO* (si) in Q65 was 13 times more than those of *InCO* (ni) in TKS.

Discussion

InCO/IhCO, a candidate gene for the largest effect QTL, qIF3, for DTF

In this study, seven QTLs for DTF, *qIF1–7*, were detected in the F_2 population of Q65 and TKS (**Table 1**). *InCO/IhCO* is located near the LOD peak of the largest effect QTL, *qIF3*. *InCO* is known to the ortholog of *CO* (Liu *et al.* 2001), which is a central regulator of photoperiodism in *Arabidopsis* (Andrés and Coupland 2012). If *InCO* were *qIF3*, then *InCO/IhCO* would be expected to have polymorphisms causing functional differences between TKS and Q65. In fact, SBD causes a frame-shift in the *InCO/IhCO* CDS (**Fig. 4**, **Supplemental Fig. 8**). The expression analysis and splicing site prediction demonstrated that the transcript variant *InCO* (si) is expected to produce a protein with an intact CCT domain in the Q65 allele (**Fig. 6**, **Supplemental Fig. 8**). Actually, *InCO* (ni) was earlier thought to be a transcript without introns and encoding the functional InCO protein (Liu *et al.* 2001), but it appears to be a minor transcript (**Figs. 4**, **6**). Although the splicing-variant *InCO* (ni) of TKS allele encodes functional CONSTANS-like protein (Liu *et al.* 2001), the expression level of TKS *InCO* (ni) is much less than that of Q65 *InCO* (si) (**Fig. 6B**). Reportedly, the expression levels of *CONSTANS* affect the flowering time in *Arabidopsis* (Rosas *et al.* 2014). Therefore, the TKS allele of *InCO* might be defective because of the frame shift caused by the SBD. For that reason, we designate the TKS/Violet type defective allele as *inco-1* and the putative ancestral allele without the SBD as *InCO-2*.

In addition to differences in the expression levels, the amino acid sequence encoded by TKS *InCO* (ni) differs from that encoded by Q65 *InCO* (si) (**Supplemental Fig. 8**). In TKS *InCO* (ni), three nonsynonymous substitutions are present, and due to alternative splicing, the region corresponding to 26 amino acids in the Q65 *InCO* (si) protein is replaced by a distinct 17-amino-acid sequence (**Supplemental Fig. 8**). Although both proteins retain key motifs such as the N-terminal B-box-type zinc fingers and the C-terminal CCT domain (**Supplemental Fig. 8**), their predicted three-dimensional structures differ substantially (Jumper *et al.* 2021). The Violet *InCO* (ni), which shares the same sequence as TKS *InCO* (ni), has been reported to complement the *co* mutant of *Arabidopsis* and promote flowering (Liu *et al.* 2001). However, *I. nil* is a short-day plant, and *InCO* is predicted to function analogously to *Hd1* in rice, acting as a flowering repressor under long-day conditions (Yano *et al.* 2000). Therefore, whether the protein encoded by TKS *InCO* (ni) is fully functional remains unclear, and further investigation using *I. nil* will be necessary to clarify the functions of transcript variants in *InCO/IhCO*.

The amino acid sequence encoded by *InCO* (si) of the African accession Q63 is identical to that of Q65 *InCO* (si), except for the asparagine–proline and asparagine repeat regions (data not shown). Considering that Q63 and Q65 belong to different species and are genetically distant (Ly *et al.* 2012), the InCO/IhCO amino acid sequence is likely subject to strong functional constraints. In contrast, the presence of three nonsynonymous substitutions between the Q65 and TKS alleles imply that the TKS allele of *InCO* might have experienced relaxed functional constraints due to loss of function.

The allelic difference of InCO/IhCO corresponds with the effects of qIF3 on DTF

If *InCO/IhCO* were *qIF3*, the phenotypic effects expected from the genotypes of *InCO/IhCO* on the DTF are assumed to correspond to the phenotypic effect of *qIF3*. The Q65 allele of *qIF3* has the effect of increasing DTF, whereas the TKS allele of *qIF3* has the effect of decreasing DTF (**Table 1**, **Supplemental Fig. 4**). Therefore, if *InCO/IhCO* were *qIF3*, then it can be inferred that *InCO/IhCO* allele without the SBD would increase DTF; also, *inco-1* allele with SBD would decrease DTF. This inference corresponds with results showing that the accessions bearing *inco-1* tend to flower earlier than those bearing the *InCO/IhCO* allele without the SBD, except Q65 (**Table 2**). Among the strains examined for this study, Q65 flowers the earliest, but it has the *IhCO* allele without the SBD (**Table 2**). The fact that Q65 flowers the earliest among accessions examined for this study does not contradict the notion that the *InCO/IhCO* allele without the SBD has an effect of delaying flowering. If *InCO/IhCO* were *qIF3*, then the Q65 allele, that is the *IhCO* allele without the SBD, would also exert a delaying effect on flowering because the Q65 allele of *qIF3* has the effect of increasing DTF (**Table 1**, **Supplemental Fig. 4**). Consequently, the allelic differences in the structure and the predicted effect for DTF of *InCO/IhCO* can well explain the allelic differences of *qIF3*.

In rice, dysfunctional alleles of *Hd1* (*hd1*), the rice ortholog of *CONSTANS*, are known to reduce photoperiod sensitivity. Moreover, they have the effect of promoting heading in field conditions (Ebana *et al.* 2011, Fujino *et al.* 2019, Hori *et al.* 2016, Mo *et al.* 2021, Yano *et al.* 2000). The early flowering tendency of rice cultivars with *hd1* corresponds with that of *I. nil* varieties with *inco-1* (**Table 2**). The photosensitivity of crops with ancestors originating from tropical regions, which are classified as short-day plants, tend to be reduced or lost during domestication and expansion to high-latitude areas (Lin *et al.* 2021). The *I. nil* varieties with *inco-1* were found exclusively in Asia but not in the Americas, the origin of *I. nil*, and Africa. Consequently, *inco-1* might have emerged in Asia, and might have contributed to the spread of *I. nil* across temperate Asia by reducing its photoperiod sensitivity.

Genetic mechanism for the early flowering of Q65

The fact that Q65 was the earliest flowering among the strains investigated for this study (**Table 2**) despite having

the ancestral allele of *InCO/IhCO* implies that Q65 possesses a mechanism for early flowering that is distinct from that of Asian *I. nil* strains. Genes other than *IhCO* might be responsible for causing Q65 to flower early.

Seven QTLs for DTF were detected in this study. Among the seven QTLs, the Q65 allele of *qIF1*, *qIF4*, *qIF5* and *qIF6* have the effect of reducing DTF and enhancing flowering (**Table 1**, **Supplemental Figs. 4**, **5**). In addition to these QTLs, two interactions also reduced DTF when both QTLs were homozygous for the Q65 allele (**Supplemental Fig. 6C**, **6D**). However, the effects of these QTLs are not stable enough to be detected in both 2011 and 2012, and were not high enough to fully explain the early flowering of Q65 (**Table 1**, **Supplemental Figs. 4**, **5**). Therefore, additional genetic studies using suitable experimental lines might be necessary to elucidate the causal genetic mechanism of the early flowering in Q65.

In rice, the combination of the loss of function of two genes, *Ghd7* and *Osppr37*, results in extremely early flowering. Given this genetic background, *Hd1* has been reported to promote earlier heading (Fujino *et al.* 2019). Similarly, in Q65, the loss of function of multiple genes other than *IhCO* can be presumed to contribute to early flowering.

Polymorphism in the 5'-upstream regulatory region of InCO/IhCO

Insertion of a SINE-like retrotransposon, which does not exist in TKS allele of *InCO/IhCO*, was observed in 5′-flanking region of Q65 allele (**Fig. 3**, **Supplemental Fig. 7**). SINEs are known to cause changes in the chromatin structure and to affect gene expression (Elbarbary *et al.* 2016). The expression levels of Q65 allele of *InCO/IhCO* are greater than those of TKS (**Fig. 6**). Therefore, structural differences and the SINE-like sequence insertion upstream of Q65 allele (**Supplemental Fig. 7**) might affect the expression level of *InCO/IhCO*.

An intron-containing InCO/IhCO transcript variant, InCO (li)

In both Q65 and TKS, *InCO* (li) exhibits the highest expression level among the three splicing variants, although it includes an intron sequence and encodes truncated protein without CCT domain (Liu *et al.* 2001) (**Fig. 6**). In *Arabidopsis*, an intron-containing *CO* transcript variant, *COβ*, also encodes a truncated protein without CCT domain caused by premature stop codon. The COβ protein interacts with the functional form of CO protein, COα, and reduces its stability (Gil *et al.* 2017). Therefore, the InCO (li) protein might also interact with the functional InCO/IhCO protein and might affect *InCO/IhCO* functions. However the expression level of *COβ* is less than *COα* (Gil *et al.* 2017). Therefore, the highest expression level of *InCO* (li) among splicing variants is a unique and interesting feature of *InCO/IhCO*.

Conclusion

This study suggests that the TKS allele of *InCO*, a candidate of the most significant QTL for DTF, *qIF3*, is likely dysfunctional due to the SBD. In tropical-origin SD plants like rice, it is known that a loss-of-function mutation in the *Hd1* enhances flowering. Similarly, the loss of function in *InCO* might promote flowering in *I. nil*. Accessions carrying the same SBD with the TKS allele tend to flower earlier, and within the accessions analyzed, those carrying the SBD were suggested to originate from temperate regions of Asia. Based on these results, we hypothesize that the SBD in *InCO* is promoting earlier flowering in mid-latitudes and enabling *I. nil*, which originated in the tropical regions of the Americas, to adapt to temperate Asia.

Author Contribution Statement

Conceptualization: HK and TK; resources provision: EN and AH; mapping population development: EN; DNA marker development: TI, HK, HF, SS, and SI; investigation: HK, TI, KE, and TK; writing–original draft preparation: HK and TK; writing–review and editing: TK, EH, and AH; supervision: AH, EN, MO, and NW; project administration: TK; funding acquisition: TK and MO. All authors have read and agreed to the published version of the manuscript.

Acknowledgments

This work was partially supported by JSPS KAKENHI Grant Number 18K05569. This work was also partially supported by the Cooperative Research Grant of the Plant Transgenic Design Initiative (PtraD) at the Gene Research Center, University of Tsukuba.

Literature Cited

Andrés, F. and G. Coupland (2012) The genetic basis of flowering responses to seasonal cues. Nat Rev Genet 13: 627–639.

Austin, D.F., K. Kitajima, Y. Yoneda and L. Qian (2001) A putative tropical American plant, *Ipomoea nil* (Convolvulaceae), in pre-Columbian Japanese art. Econ Bot 55: 515–527.

Broman, K.W., H. Wu, Ś. Sen and G.A. Churchill (2003) R/qtl: QTL mapping in experimental crosses. Bioinformatics 19: 889–890.

Cao, S., R.W. Kumimoto, N. Gnesutta, A.M. Calogero, R. Mantovani and B.F. Holt (2014) A distal *CCAAT*/NUCLEAR FACTOR Y complex promotes chromatin looping at the *FLOWERING LOCUS T* promoter and regulates the timing of flowering in *Arabidopsis*. Plant Cell 26: 1009–1017.

Ebana, K., T. Shibaya, J. Wu, K. Matsubara, H. Kanamori, H. Yamane, U. Yamanouchi, T. Mizubayashi, I. Kono, A. Shomura *et al.* (2011) Uncovering of major genetic factors generating naturally occurring variation in heading date among Asian rice cultivars. Theor Appl Genet 122: 1199–1210.

Edwards, C.E., T.L. Parchman and C.W. Weekley (2012) Assembly, gene annotation and marker development using 454 floral transcriptome sequences in *Ziziphus celata* (Rhamnaceae), a highly endangered, Florida endemic plant. DNA Res 19: 1–9.

Elbarbary, R.A., B.A. Lucas and L.E. Maquat (2016) Retrotransposons as regulators of gene expression. Science 351: aac7247.

Fujino, K., U. Yamanouchi, Y. Nonoue, M. Obara and M. Yano (2019) Switching genetic effects of the flowering time gene *Hd1* in LD conditions by *Ghd7* and *OsPRR37* in rice. Breed Sci 69: 127–132.

Fukuoka, H., K. Miyatake, S. Negoro, T. Nunome, A. Ohyama and H. Yamaguchi (2008) Development of a routine procedure for single nucleotide polymorphism marker design based on the T_m-shift genotyping method. Breed Sci 58: 461–464.

Galli, G., H. Hofstetter and M.L. Birnstiel (1981) Two conserved sequence blocks within eukaryotic tRNA genes are major promoter elements. Nature 294: 626–631.

Gil, K.E., M.J. Park, H.J. Lee, Y.J. Park, S.H. Han, Y.J. Kwon, P.J. Seo, J.H. Jung and C.M. Park (2017) Alternative splicing provides a proactive mechanism for the diurnal CONSTANS dynamics in Arabidopsis photoperiodic flowering. Plant J 89: 128–140.

Hayama, R., S. Yokoi, S. Tamaki, M. Yano and K. Shimamoto (2003) Adaptation of photoperiodic control pathways produces short-day flowering in rice. Nature 422: 719–722.

Hayama, R., B. Agashe, E. Luley, R. King and G. Coupland (2007) A circadian rhythm set by dusk determines the expression of *FT* homologs and the short-day photoperiodic flowering response in Pharbitis. Plant Cell 19: 2988–3000.

Hebsgaard, S.M., P.G. Korning, N. Tolstrup, J. Engelbrecht, P. Rouze and S. Brunak (1996) Splice site prediction in *Arabidopsis thaliana* pre-mRNA by combining local and global sequence information. Nucleic Acids Res 24: 3439–3452.

Higuchi, Y., K. Sage-Ono, R. Sasaki, N. Ohtsuki, A. Hoshino, S. Iida, H. Kamada and M. Ono (2011) Constitutive expression of the *GIGANTEA* ortholog affects circadian rhythms and suppresses one-shot induction of flowering in *Pharbitis nil*, a typical short-day plant. Plant Cell Physiol 52: 638–650.

Hori, K., K. Matsubara and M. Yano (2016) Genetic control of flowering time in rice: integration of Mendelian genetics and genomics. Theor Appl Genet 129: 2241–2252.

Hoshino, A., V. Jayakumar, E. Nitasaka, A. Toyoda, H. Noguchi, T. Itoh, T. Shin-I, Y. Minakuchi, Y. Koda, A. Nagano *et al.* (2016a) Genome sequence and analysis of the Japanese morning glory *Ipomoea nil*. Nat Commun 7: 13295.

Hoshino, A., Y. Yoneada and T. Kuboyama (2016b) A *Stowaway* transposon disrupts the *InWDR1* gene controlling flower and seed coloration in a medicinal cultivar of the Japanese morning glory. Genes Genet Syst 91: 37–40.

Izawa, T., T. Oikawa, N. Sugiyama, T. Tanisaka, M. Yano and K. Shimamoto (2002) Phytochrome mediates the external light signal to repress *FT* orthologs in photoperiodic flowering of rice. Genes Dev 16: 2006–2020.

Jumper, J., R. Evans, A. Pritzel, T. Green, M. Figurnov, O. Ronneberger, K. Tunyasuvunakool, R. Bates, A. Žídek, A. Potapenko *et al.* (2021) Highly accurate protein structure prediction with AlphaFold. Nature 596: 583–589.

Kojima, S., Y. Takahashi, Y. Kobayashi, L. Monna, T. Sasaki, T. Araki and M. Yano (2002) *Hd3a*, a rice ortholog of *Arabidopsis FT* gene, promotes transition to flowering downstream of *Hd1* under short-day condition. Plant Cell Physiol 43: 1096–1105.

Larkin, M.A., G. Blackshields, N.P. Brown, R. Chenna, P.A. McGettigan, H. McWilliam, F. Valentin, I.M. Wallace, A. Wilm, R. Lopez *et al.* (2007) Clustal W and Clustal X ver. 2.0. Bioinformatics 23: 2947–2948.

Li, H., J. Ruan and R. Durbin (2008) Mapping short DNA sequencing reads and calling variants using mapping quality scores. Genome Res 18: 1851–1858.

Liew, M., R. Pryor, R. Palais, C. Meadows, M. Erali, E. Lyon and C. Wittwer (2004) Genotyping of single-nucleotide polymorphisms by high-resolution melting of small amplicons. Clin Chem 50: 1156–1164.

Lin, X., C. Fang, B. Liu and F. Kong (2021) Natural variation and artificial selection of photoperiodic flowering genes and their applications in crop adaptation. aBIOTECH 2: 156–169.

Liu, J., J. Yu, L. McIntosh, H. Kende and J.A.D. Zeevaart (2001) Isolation of a *CONSTANS* ortholog from *Pharbitis nil* and its role in flowering. Plant Physiol 125: 1821–1830.

Ly, T., H. Fukuoka, A. Otaka, A. Hoshino, S. Iida, E. Nitasaka, N. Watanabe and T. Kuboyama (2012) Development of EST-SSR markers of *Ipomoea nil*. Breed Sci 62: 99–104.

Meng, L., H. Li, L. Zhang and J. Wang (2015) QTL IciMapping: Integrated software for genetic linkage map construction and quantitative trait locus mapping in biparental populations. Crop J 3: 269–283.

Mo, Y., C.M. Lee, H.M. Park, S.K. Ha, M.J. Kim, J. Kwak, H.S. Lee, J.H. Lee and J.U. Jeung (2021) *Hd1* allele types and their associations with major agronomic traits in Korean rice cultivars. Plants (Basel) 10: 2408.

Putterill, J., F. Robson, K. Lee, R. Simon and G. Coupland (1995) The *CONSTANS* gene of Arabidopsis promotes flowering and encodes a protein showing similarities to zinc finger transcription factors. Cell 80: 847–857.

Rosas, U., Y. Mei, Q. Xie, J.A. Banta, R.W. Zhou, G. Seufferheld, S. Gerard, L. Chou, N. Bhambhra, J.D. Parks *et al.* (2014) Variation in *Arabidopsis* flowering time associated with *cis*-regulatory variation in *CONSTANS*. Nat Commun 5: 3651.

Rozen, S. and H. Skaletsky (2000) Primer3 on the WWW for general users and for biologist programmers. *In*: Misener, S. and S.A. Krawetz (eds.) Bioinformatics methods and protocols: Methods in molecular biology. Humana Press, Totowa, NJ, pp. 365–386.

Sato, S., S. Isobe, E. Asamizu, N. Ohmido, R. Kataoka, Y. Nakamura, T. Kaneko, N. Sakurai, K. Okumura, I. Klimenko *et al.* (2005) Comprehensive structural analysis of the genome of red clover (*Trifolium pratense* L.). DNA Res 12: 301–364.

Takeno, K. (2016) Stress-induced flowering: The third category of flowering response. J Exp Bot 67: 4925–4934.

Tamaki, S., S. Matsuo, H.L. Wong, S. Yokoi and K. Shimamoto (2007) Hd3a protein is a mobile flowering signal in rice. Science 316: 1033–1036.

Voorrips, R.E. (2002) MapChart: Software for the graphical presentation of linkage maps and QTLs. J Hered 93: 77–78.

Wang, J., K. Chuang, M. Ahluwalia, S. Patel, N. Umblas, D. Mirel, R. Higuchi and S. Germer (2005) High-throughput SNP genotyping by single-tube PCR with T_m-shift primers. Biotechniques 39: 885–893.

Yano, M., Y. Katayose, M. Ashikari, U. Yamanouchi, L. Monna, T. Fuse, T. Baba, K. Yamamoto, Y. Umehara, Y. Nagamura *et al.* (2000) *Hd1*, a major photoperiod sensitivity quantitative trait locus in rice, is closely related to the Arabidopsis flowering time gene *CONSTANS*. Plant Cell 12: 2473–2483.

Yoneda, Y. and Y. Takenaka (1981) Genshoku asagao kensaku zukan (Natural-Color Illustrated monograph of Japanese morning glory), 2nd edn. Hokuryukan, Tokyo, pp. 50–58 (in Japanese).

Zheng, C.C., D. Potter and S.D. O'Neill (2009) Phytochrome gene expression and phylogenetic analysis in the short-day plant *Phabitis nil* (Convolvulaceae): differential regulation by light and an endogenous clock. Am J Bot 96: 1319–1336.